

Low-noise $\text{YBa}_2\text{Cu}_3\text{O}_7$ rf SQUID magnetometer

Yi Zhang, H.-M. Mück, K. Herrmann, J. Schubert, W. Zander, A. I. Braginski, and C. Heiden

Institut für Schicht und Ionentechnik (ISI), Forschungszentrum Jülich (KFA), Postfach 1913, D-W5170 Jülich, Germany

(Received 20 September 1991; accepted for publication 21 November 1991)

A superconducting quantum interferometer device (SQUID) electronics with tank frequencies near 150 MHz was constructed to enhance the rf SQUID sensitivity. By these means we characterized our $\text{YBa}_2\text{Cu}_3\text{O}_7$ thin-film rf SQUIDs with step-edge junctions immersed in liquid N_2 . We obtained transfer function values of over $40 \mu\text{V}/\Phi_0$, at a 50Ω input impedance, for both hysteretic and dispersive mode of rf SQUID operation. The rms white and $1/f$ flux noise levels were significantly lower than at the tank frequency of 20 MHz. The best magnetic field sensitivity at 77 K was $0.9 \text{ pT/Hz}^{1/2}$, and the energy resolution $1.4 \times 10^{-28} \text{ J/Hz}$, down to 0.3 Hz.

We have been investigating rf SQUIDs with step-edge junctions fabricated from epitaxial $\text{YBa}_2\text{Cu}_3\text{O}_7$ (YBCO) thin films and capable of operating at 77 K. Such rf SQUIDs were first reported by Daly *et al.*¹ and Cui *et al.*² Several groups of authors have also been investigating dc SQUIDs with step-edge junctions.³⁻⁶ Daly *et al.*¹ and Yoshii *et al.*³ observed that step-edge-junction devices are capable of relatively low $1/f$ noise performance. The observed noise level was, in fact, comparable to that of dc SQUIDs with grain-boundary junctions on bicrystal substrates.⁷ Our study of single step-edge microbridges has shown that their characteristics are very similar to those of grain-boundary junctions.⁸ We have also shown there that the $1/f$ noise of our rf SQUIDs, observed below 100 Hz, was dominated by the $1/f$ noise in these junctions, as in the bicrystal dc SQUID.

Here we report on recent results of our work aimed at constructing a low $1/f$ noise rf SQUID multipurpose magnetometer operating at 77 K. For comparison of sensitivity data we refer to the recently published data of an integrated "flip-chip" dc SQUID magnetometer with a multi-turn coil flux transformer.⁹

The fabrication of our step-edge junctions and rf SQUIDs was described in Refs. 2 and 8. The test chips used here consisted of epitaxial YBCO films pulsed-laser deposited on $10 \times 10 \text{ mm}$ (100) SrTiO_3 substrates having ion-beam etched steps and pits at appropriate locations. The film thicknesses, d , and the step heights (pit depths), h , were between 130 and 200 nm with the d/h ratio equal either 1 or $2/3$. The central area of the test chip was occupied by four rf SQUID washers arranged into a square with 0.5 mm spacings between them. Each $1.4 \times 1.4 \text{ mm}$ washer contained two step-edge junctions in series since its $10 \mu\text{m}$ long microbridge was positioned over a local $5 \mu\text{m}$ wide pit in the substrate. In a fabricated chip, the microbridge width was typically $2.0\text{--}2.5 \mu\text{m}$. Each washer's hole was $100 \times 100 \mu\text{m}$ corresponding to a SQUID geometrical inductance of approximately $L_g = 125 \text{ pH}$. Four single microbridges over steps, and a reference bridge without any step, were also positioned on the chip. The I - V characteristics of step-edge junctions on the chip were of RSJ-type.⁸

At 77 K, their product of critical current and normal resistance was $I_c R_n < 100 \mu\text{V}$.

In our past work, we used standard rf-SQUID electronics, e.g., the BTI model 330 operating at about 20 MHz. To improve the rf SQUID sensitivity, one can increase the tank frequency, ω_{rf} . The value of the transfer function, $dV/d\Phi = \omega_{\text{rf}} L_T / M$, where L_T is the inductance of the tank circuit and M the mutual inductance, is thus increased and the intrinsic noise decreased.¹⁰ To this effect, we constructed a read-out electronic circuit operating at an, approximately, 150 MHz tank frequency. To permit one to use arbitrary transmission line lengths, a 50Ω input impedance was chosen. The higher impedance of the tank circuit was matched to the 50Ω line by means of a capacitive tap, as shown in Fig. 1. The values of tank circuit inductances and capacitances are indicated there. The value of C_2 , chosen to give a high return loss, was determined experimentally using a network analyzer. A return loss of 10 db or better was sufficient to obtain an optimum SQUID signal. The rf choke L' made it possible for dc currents of the flux-locked loop to bypass C_1 .

A free running variable frequency (120–180 MHz) oscillator was used since the resonant frequency of the tank circuit could not be changed. For different SQUIDs, a different value of C_2 had to be chosen. The tank circuit quality factor was $Q = 40\text{--}60$, as measured with a network analyzer. This was a factor of about two higher than in 20 MHz tank circuits. The improvement in Q was due to the fact that the transmission line capacitance does not add to that of the tank circuit, thus resulting in a more favorable L/C ratio. Additionally, a somewhat larger wire diameter was used in the tank circuit coil, thus reducing ohmic losses. No thermal noise generated in this normal-conducting coil could be observed. Following a broadband 60 db signal amplification, synchronous detection was used instead of the conventional envelope detection, in order to reduce the overall noise bandwidth of the read-out electronics. A comparison of sensitivity and noise data obtained with this and the conventional 20 MHz electronics will be shown below.

We tested the 150 MHz circuit by measuring several rf

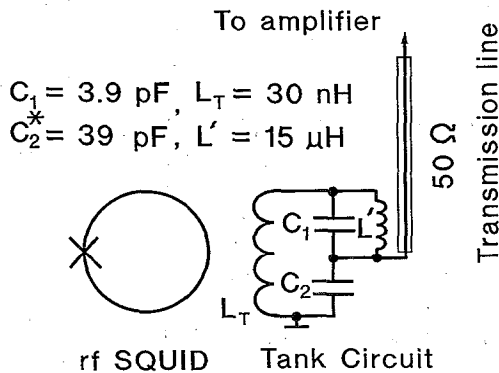


FIG. 1. A schematic diagram of the 150 MHz tank circuit. The C_2^* represents a capacitance value determined experimentally for each rf SQUID sample.

SQUIDS having at 77 K a $\beta_L = 2\pi I_c L_s / \Phi_0 < 1$ and output signals so low that at 20 MHz the flux-locked loop mode in the BTI 330 electronics could not function. At 150 MHz, however, we obtained $dV/d\Phi > 40 \mu\text{V}/\Phi_0$, as in SQUIDS with $\beta_L > 1$. Operation in the flux-locked loop mode presented no difficulties. Indeed, at 150–160 MHz, with the measured mutual and tank inductances of $M = 1 \text{ nH}$ and $L_T = 0.3 \mu\text{H}$, we have fulfilled the requirement for an optimum $dV/d\Phi$: $k^2 Q \gg 1$, where $k = M/(L_T L_s)^{1/2}$ is the coupling coefficient.¹¹ This requirement could not be met at 20 MHz. Figure 2 shows the typical rf SQUID output signal at 150 MHz tank frequency for two modulating field intensities. Note that the signal envelope exhibits a very weak

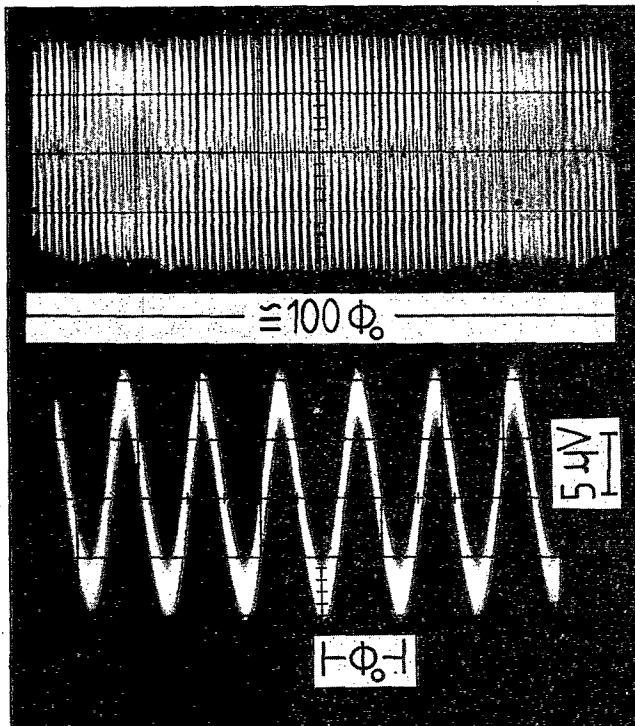


FIG. 2. Typical output signal of rf SQUID at 77 K and two modulating field intensities. Measurement bandwidth is, approximately, 200 kHz.

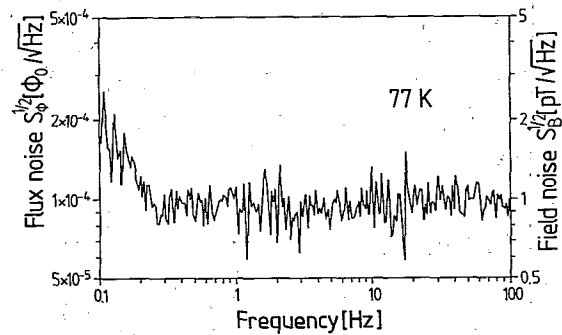


FIG. 3. Flux and field noise spectrum of a low $1/f$ noise rf SQUID with 2 step-edge junctions in series, measured at the tank frequency of 150 MHz.

modulation with a period of, approximately, $100\Phi_0$. This modulation period corresponds to that of an inhomogeneous step-edge junction which can be represented by an equivalent dc SQUID with a loop area of the order of $1 \mu\text{m}^2$ and a corresponding field focusing coefficient of the chip structure (discussed below). The weakness of modulation indicates that the double step-edge junction itself was relatively homogeneous.

Measurements of flux noise spectra $S_\Phi(f)$ at 77 K have been performed using the HP3562A Dynamic Signal Analyzer, whereby the rigidly mounted SQUID chip probe was immersed in liquid nitrogen contained within a mu-metal-shielded, low-self-noise fiberglass dewar. Spectral data were averaged over 5–10 spectral samples so that the measurement times for one spectrum were up to 2 h. We stress the importance of mechanical stability of such a setup since in inhomogeneous magnetic fields any motion or vibration due, e.g., to boiling N_2 gives rise to an additional flux noise at low frequencies. Using the 150 MHz electronics, we obtained for all tested SQUIDS a white noise rms level between 0.8×10^{-4} and $1.5 \times 10^{-4} \Phi_0 \text{Hz}^{-1/2}$. In most of the tested SQUIDS, we found the $1/f$ noise submerged by white noise at frequencies of 1 Hz and above. Figure 3 shows a noise spectrum of a sample exhibiting a particularly low $1/f$ noise. The crossover from $1/f$ to white noise of $8\text{--}9 \times 10^{-5} \Phi_0 \text{Hz}^{-1/2}$ occurs at 0.3 Hz, approximately. The corresponding energy resolution at this frequency is $1.4 \times 10^{-28} \text{ J/Hz}$.

We have compared flux noise levels in hysteretic SQUID samples ($\beta_L > 1$) at tank frequencies of $\omega_{\text{rf}}/2\pi = 20$ and 160 MHz. An example of results is shown in Fig. 4, for a sample different from that of Fig. 3. In a variety of investigated samples, the white noise $S_\Phi^{1/2}(f)$ at 160 MHz was lower than at 20 MHz by a factor of 2–4. The $1/f$ noise was similarly reduced. It follows from rf SQUID noise theory¹⁰ that $S_\Phi^{1/2}(f)$ for a statistically random noise should scale with $1/\omega_{\text{rf}}^{1/2}$. We can thus expect the white noise $S_\Phi^{1/2}(f)$ measured at 160 MHz to be 2.8 times lower than at 20 MHz. The experimental results are in a reasonable agreement with this expectation. A similar behavior of $1/f$ noise suggests that it is also a statistically random effect. We are thus tempted to believe that the $1/f$

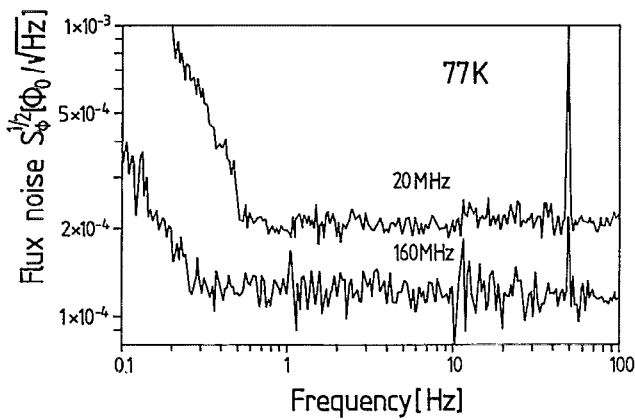


FIG. 4. Comparison of flux noise spectra in a rf SQUID structure (different from that of Fig. 3) measured at tank frequencies of 20 and 160 MHz.

noise is dominated by random current and resistivity fluctuations in the step-edge junctions, similar as in dc SQUIDs with grain boundary junctions on bicrystal substrates.¹² The sample-to-sample scatter in $1/f$ $S_{\Phi}^{1/2}(f)$ scaling was larger than in white noise scaling. This could be due to the reduction in measurement accuracy at the low end of the noise spectrum, i.e. between 1 and 0.1 Hz, caused by insufficient averaging.

By a direct calibration with external single-turn coils, the field-flux transformation coefficient of our SQUIDs was determined to be 9.8×10^{-9} T/ Φ_0 . The resulting field noise calibration is also given in Fig. 3. At 77 K, the white-noise-limited field sensitivity of the SQUID of Fig. 3 was 0.9 pTHz $^{-1/2}$ down to 0.3 Hz. At frequencies below 10 Hz, which are important, e.g., in biomagnetic applications, this compared rather favorably with the field sensitivity of the integrated dc SQUID magnetometer.⁹ This sensitivity was 0.6 pTHz $^{-1/2}$ at 10 Hz and proportional to $1/f^{1/2}$ up to, at least, 100 Hz. At that frequency, the dc SQUID magnetometer was thus by a factor of 3–4 more sensitive than ours. We realize that also at low frequencies the sensitivities of large focusing washer SQUIDs will, ultimately, not be able to match those of integrated SQUIDs with multiturn input coils. However, we were able to show that a technically meaningful sensitivity level can also be attained in simple planar rf SQUID structures.

The effective area of the SQUID pickup loop was found to be $A_{\text{eff}} = 2.1 \times 10^5$ μm^2 , a factor of 21 higher than

that of the geometrical area $A = 10^4$ μm^2 . This flux focusing coefficient was 40% higher than that calculated for an isolated single washer.¹³ The stronger than calculated focusing effect was caused by the neighboring SQUID and bridge structures on the chip. Measurement on two single washers which were cut out from the chip showed an excellent agreement with calculations. Although flux focusing increases only slowly with the washer area, this agreement permits us to expect flux focusing coefficients of over 100 for a single 10×10 mm 2 chip, and even higher with adjoining thin-film focusing elements.

In conclusion, using step-edge YBCO junctions and a tank frequency of, approximately, 150 MHz, we demonstrated the feasibility of a simple rf-SQUID magnetometer operating at 77 K with a sensitivity of up to 0.9 pTHz $^{-1/2}$ at 0.3 Hz. The simplicity of planar rf-SQUID structures makes our approach attractive. The sensitivity of such planar rf SQUIDs could be further increased, by up to an order of magnitude, through further increases in both the tank frequency and the focusing structure area.

We acknowledge a partial support of the BMFT Consortium "First Applications of HTS in Micro- and Cryoelectronics."

¹ K. P. Daly, W. D. Dozier, J. F. Burch, S. B. Coons, R. Hu, C. E. Platt, and R. W. Simon, Appl. Phys. Lett. **58**, 543 (1991).

² G. Cui, Y. Zhang, K. Herrmann, Ch. Buchal, J. Schubert, W. Zander, A. I. Braginski, and C. Heiden, Supercond. Sci. Technol. **4** S130 (1991).

³ M. Yoshii, J. Kita, O. Nakatsu, and Y. Yamada, Jpn. J. Appl. Phys. **30**, L587 (1991).

⁴ M. Siegel, F. Schmidl, K. Zach, E. Heinz, J. Borck, W. Michalke, and P. Seidel, Physica C **180**, 288 (1991).

⁵ K. Enpuku, J. Udomoto, T. Kisu, and K. Yoshida, Extended Abstracts of the Third International Superconductive Electronics Conference (ISEC '91), University of Strathclyde, Glasgow 1991, p. 403.

⁶ C. W. Yuan, A. B. Berezin, and A. L. de Lozanne, Bull. APS **36**, 877 (1991).

⁷ R. Gross and B. Mayer, Physica C **180**, 235 (1991).

⁸ K. Herrmann, Y. Zhang, H.-M. Mück, J. Schubert, W. Zander, and A. I. Braginski, Supercond. Sci. Technol. **4**, 583 (1991).

⁹ A. H. Miklich, J. J. Kingston, F. C. Wellstood, J. Clarke, M. S. Colclough, K. Char, and G. Zaharchuk, Appl. Phys. Lett. **59**, 988 (1991); and Nature **352**, 483 (1991).

¹⁰ L. D. Jackel and R. A. Buhrman, J. Low Temp. Phys. **19**, 201 (1975).

¹¹ M. Simmond and H. Parker, J. Appl. Phys. **42**, 38 (1971).

¹² M. Kawasaki, P. Chaudhari, and A. Gupta (IBM), Phys. Rev. Lett. (to be published).

¹³ M. B. Ketchen, W. J. Gallagher, A. W. Kleinsasser, S. Murphy, and J. R. Clem, in *SQUID'85 - Superconducting Interference Devices and their Applications*, edited by H. D. Hahlbohm and H. Lübbig (de Gruyter, Berlin, 1985), p. 865.